HEFAT2008
6th International Conference on Heat Transfer, Fluid Mechanics and Thermodynamics
University of Pretoria,
Pretoria, South Africa
Paper number: FT1

EXPERIMENTAL AND PIV-METHOD STUDIES OF LEAN MIXTURE FLAMES, FOCUSED ON EXTINCTION DURING ITS PROPAGATION IN A STANDARD TUBE RESULTING FROM FLAME STRETCHING

Fodemski T.R.* and Górecki G.
*Author for correspondence
Department of Heat Technology and Refrigeration
Technical University of Łódź, 90-924 Łódź, ul. Stefanowskiego 1/15, Poland
e-mail: *fodemski@p.lodz.pl*

ABSTRACT

The main goal of this work is to determine experimentally local stretch rate distribution along limit methane/air and propane/air flames – using Particle Image Velocimetry (PIV) method. It allows to obtain necessary moving flame velocity fields in a standard flammability column and, also, to recognize the flame structures. For this purpose each mixture was seeded with MgO particles (of known size) before entering the tube (column) – using a special system. The amount of seeds in the mixture, their dispersion system and the laser power producing a sheet of light penetrating the column – were carefully chosen (not to disrupt the combustion or flame propagation in it). After learning process, finally it allowed to obtain the good quality velocity field images in the region concern – acceptable for further processing. The methodology developed for these experiments proved to be reliable and able to supply analyses with repeatable data. On the basis of performed experiments it was possible to derive the flame stretch rate which causes its extinction for both mixtures.

INTRODUCTION

Lean limit mixture flame, propagating in a vertical standard tube (with rectangular 5cmx5cm or circular 5cm diameter cross-sections) was used in experiments. Two different combustible mixtures, i.e. methane-air and propane-air (referred to below as CH_4/air and C_3H_8/air) were analyzed. Following the ignition at the column bottom open end flame propagates up towards closed end. Gas concentration at which flame extinction occurs before flame reaches the top end of the standard column is referred to as a limit concentration and flame in the standard tube at this concentration is called limit flame. Experiments show that extinction of both CH_4/air and C_3H_8/air limit flames (their concentrations are 5.25% and 2.2%, respectively) in these conditions are similar. They always start at the flame tip and then spread down toward the flame skirt. Since the heat loss effect to the cold walls is negligible there, it is claimed that other reasons might be responsible for this limit flame extinction. Generalized approach has been developed by Karlovitz [1]. It involves the idea of the flame stretch rate to describe local flame front propagation and extinction and is based on the analysis of the velocity field in the mixture and in the combustion gases – close to the flame. However, there is still a need for reliable, good quality experimental results. One of the most promising method to analyze velocity fields is the PIV-method.

NOMENCLATURE

a	[m_2/s]	Thermal diffusivity
A	[m^2]	Flame surface area
c_p	[J/kg K]	Specific heat at constant pressure
H	[m]	Column height
k	[s^{-1}]	Stretch rate
D	[m^2/s]	Diffusion coefficient
Ka	[-]	Karlowitz number
L	[m]	Length or coordinate along flame
Le	[-]	Lewis number
$\dot{m}_V$	[l/h]	Volume rate of flow
Ma	[-]	Markstein number
q	[J/kmol]	Reaction heat
t	[s]	Time
T	[K]	Temperature
u_L	[m/s]	Laminar flame velocity
V	[m/s]	Velocity
X,Y,Z	[m]	Cartesian axes directions
δ	[m]	Flame thickness
λ	[W/m K]	Heat conductivity coefficient
ρ	[kg/m^3]	Density
Ω	[kmol/s·m^3]	Combustion reaction velocity

Subscripts

m	[-]	Value for mixture
M	[-]	Markstein value
A-B	[-]	Andrews and Bradley value
G-W	[-]	Gaydon and Wolfhard value
Sp	[-]	Spalding value
Zel	[-]	Zeldo'vich value
∞	[-]	Value for the laminar, not stretched plane flame

This work reports the state of project which is not completed and is, in fact, processed now. However, authors think that it is worth to publish results and conclusions already obtained.

The important features of the plane laminar flame are shown in Fig. 1 and 2 (with three zones, determined by the temperature distribution, resulting from Eq. 1 [2]).

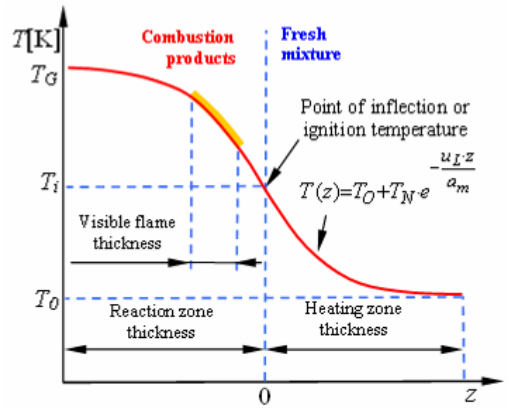

Figure 1. The laminar flame features.

The energy equation for this flame, moving with the velocity $u_{L\infty}$, has the form of the 2nd order differential equation [3]:

$$\lambda \frac{d^2T}{dz^2} - u_{L\infty} c_p \rho \frac{dT}{dz} + q\Omega = 0 \qquad (1)$$

where: *I* – zone of mixture heating, $\Omega = 0$;
II – ignition zone, $d^2T/dz^2 \approx 0$ and
III – reaction zone in final temperature i.e. $dT/dz \cong 0$

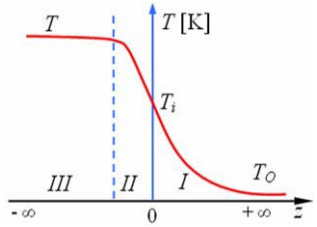

Figure 2. Three zones of plane laminar flame structure [1].

In Fig.3 an example of measured temperature profile (curve 1 determined by experimental points [2]) and, for comparison, exponential profile (defined by equation in Fig. 1) are shown.

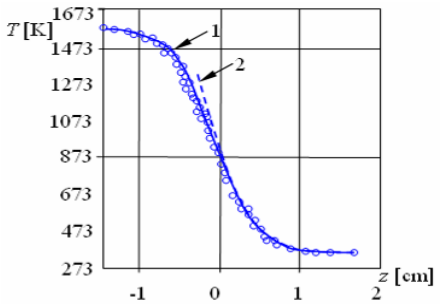

Figure 3. Temperature profiles: (1) experimental – in all zones [2]; and (2) exponential – in the heating zone.

The determination of the "flame thickness" is important. On the grounds of the Eq. 1 solution in zone *I*, Zeldo'vich [4] defined laminar flame thickness δ_{Zel}, expressed by the formula:

$$\delta_{Zel} = \frac{a_m}{u_L} = \frac{\lambda_m}{c_{pm}\rho_m u_L} \qquad (2)$$

The other proposition, by Spalding [3], defines δ_{Sp} as:

$$\delta_{Sp} = \frac{(T_G - T_O)}{(dT/dz)_{\max}} \qquad (3)$$

Flame thickness $\delta_{G\text{-}W}$, by Gaydon and Wolfhard [5], is defined as a layer from the temperature inflection point (see Fig. 1) to the point where it differs by 1% from the fresh mixture temperature.

The other flame thickness definition, $\delta_{A\text{-}B}$ (by Andrews and Bradley [6]), is based on the experimental measurements using non-invasive interferometer – allowing to determine special points A and B (see Fig. 4).

All thicknesses mentioned above are shown in Fig. 4. One can find, neglecting the temperature changes of the material parameters, that $\delta_{Sp} = 2\ \delta_{Zel}$; $\delta_{G\text{-}W} = 4.6\ \delta_{Ze}$ and, also, that the experimental $\delta_{A\text{-}B}$ value is the largest one.

The lack of unified thickness definition results in difficulty of the flame stretch rate determination (see Eqs 4 to 8 below).

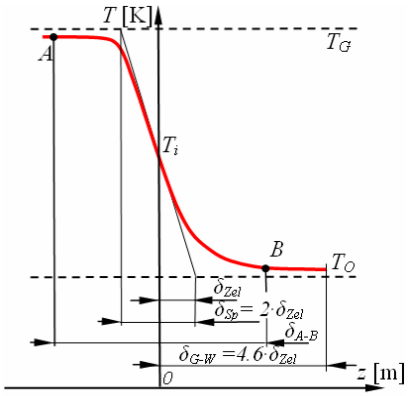

Figure 4. Different laminar flame thickness definitions .

EXPERIMENTAL SET-UP

The PIV method and equipment

The PIV Dantec® system (see Fig. 5) was used: two pulse Ng YAG lasers with maximum 50 mJ energy output, digital video camera CCD 80V60PIV/PLF Hi-Sense (1280x1024 pixels), special FlowManager® double PIV processing unit and a computer controlling all units. The maximum rate of PIV system operation was 4 measurements (4 double frames) per second. In the experiments, different physical areas of the column were recorded.

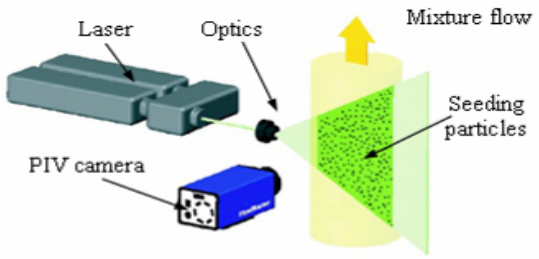

Figure 5. The PIV set-up.

The principle of this method is shown in Fig.6. Two pictures, coinciding with the presence of the "sheet laser light", are taken in a short Δt time interval and 2 pictures with the seeding particles are recorded. Knowing particle positions on both pictures (they are divided into "interrogation areas") and the Δt value – one velocity field (related to this laser light plane surface) is created and is ready for further processing. The system allows to make 4 velocity pictures per second, i.e. to obtain information how this field changes in time.

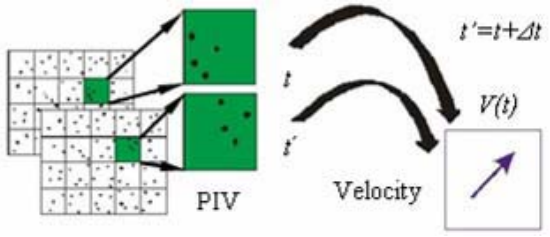

Figure 6. Principle of seeding velocity determination .

The seeding particles and mass and the flammability column

The MgO seed particles were used throughout all experiments reported in this work. The particle volume distribution is presented in Fig. 7.

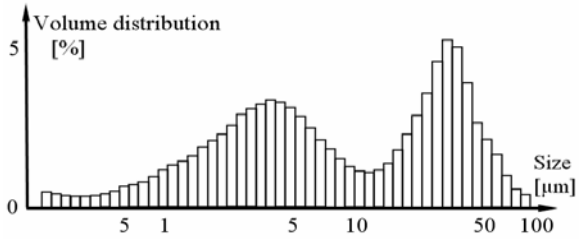

Figure 7. Volume distribution of seed particles.

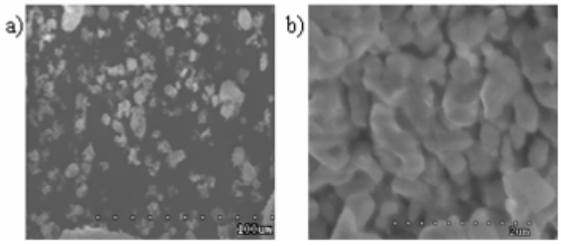

Figure 8. Microscope pictures of the MgO-seeding: (a) particles; (b) particle surface.

The microscopic analyses of the MgO particles were made using the scanning microscope Hitachi S-3000N. The observations of the particles were made before and after the experiments. No influence or sign of any effect both on the volume distribution and the particle surfaces were noticed. The latter proved that there is no chemical reaction in the combustion in which the MgO particles are involved.

In all the experiments different columns were used – two of them only for the analyses of the mixture flow with seeds and to check supply conditions and resulting from it the MgO particles distribution in columns. They showed that the top column supply is superior. The flammability columns used in combustion experiments are shown in Fig. 9. The better results of seeding distribution inside columns were achieved using the pressurized one with the shredder. It is worth mentioning that combustion in the column results in the flow of reaction products towards open bottom end, while fresh mixture between the flame and the closed top is still. This lowers the MgO particles distribution immediately below the flame front by about one order of magnitude (see Fig. 10 where, additionally, the application of the optical filter – cutting all but the laser light for the camera recording – is crucial). This is important, since the system used requires sufficient seeding particles number density for the good quality PIV picture in this region.

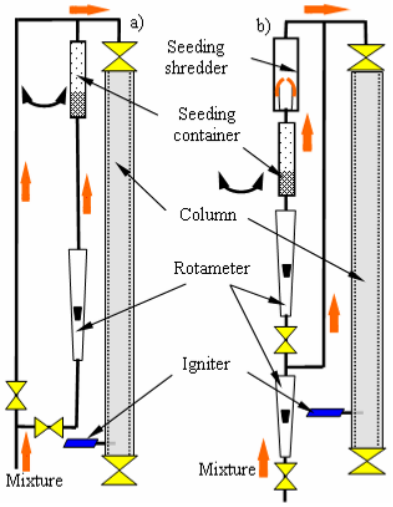

Figure 9. Flammability columns and mixture with seeding supply systems at: (a) atmospheric (b) above atmospheric pressures.

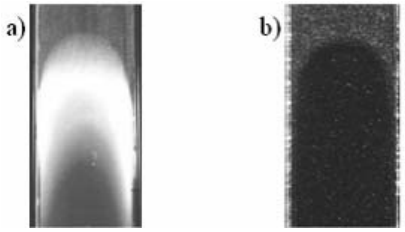

Figure 10. PIV pictures of moving flame in CH_4/air: (a) without a filter and (b) with the optical filter.

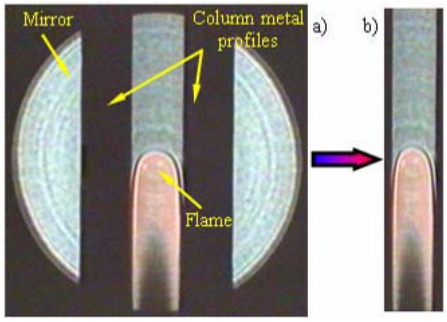

Figure 11. (a) Optical set-up of the "shadow" method flame pictures and (b) extracted part showing flame propagation in the flammability column.

The "shadow" method was also used to record flame behaviour. Fig. 11 shows its full set-up and interesting part of the flame. The analysis concentrated on pictures like the one presented in Fig.11b

helped to analyze the influence of the seeding mass amount in the standard flammability column on the flame propagation velocity in it. This velocity can be determined for any mass and compared to the one without MgO. Chosen set of pictures showing this effect (including flame colour related to the MgO mass) is shown in Fig. 12.

The adopted solution of the problem to control seeding mass in the column (when filling it using the replacement method) is actually presented in Fig. 9a and b. The total prepared gas mixture flow is divided in two parallel flows. The flow to the seed container is controlled by the rotameter. The controlled m_V mixture flow blows away seeding mass m related to this flow (relation for the practical use was established).

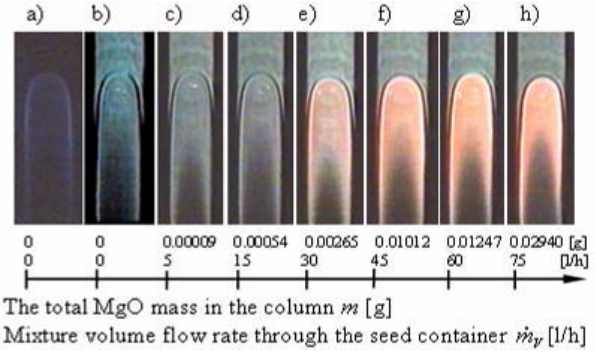

Figure 12. Influence of total seeding mass on flame velocity in flammability column 5cm×5cm×1.8m; CH_4/air mixture. Picture (a) by ordinary camera (no seeding). The "shadow" method pictures: (b) no seeding; (c÷h) with seeding.

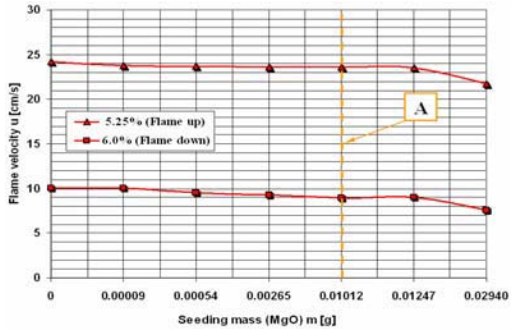

Figure 13. Influence of seeding mass on flame velocity propagation; 5cm×5cm×1m column; CH_4/air mixture.

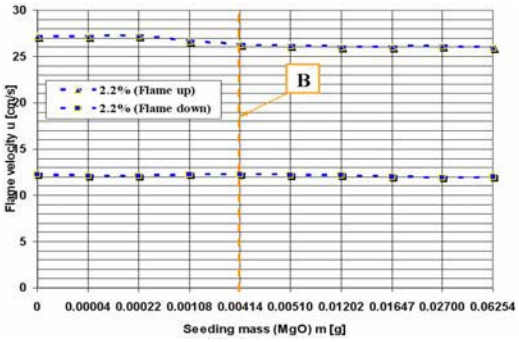

Figure 14. Influence of seeding mass on flame velocity propagation; 5cm×5cm×1m column; C_3H_8/air mixture.

Results of extensive experiments are shown in Figs 13 and 14 (they include flames moving down the column – not discussed here). For each mixture one can notice a fall in flame velocity measured when seeding mass increases. Lines A and B in figures mentioned show maximum values used in reported experiments.

The last two important experimental limitations were also analyzed. One is related to the observed but undesired lack of flame symmetry or even surface oscillations during its propagation in flammability column. The stable flame shape in columns is always symmetrical, regardless their cross-section (Fig.15 show columns with circular and rectangular cross-sections). Fig.16 a and b presents symmetrical and non-symmetrical flame shapes (see 3-D models of the latter). It was found that this non-symmetrical shape and flame behaviour results from the lack of thermal equilibrium of the column walls and the time gap between two consecutive experiments not shorter than 30 min is the practical solution.

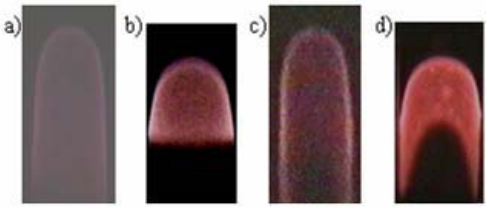

Figure 15. Pictures of stable flame propagation in mixtures with the MgO-seeding

5cm in diam.×1.8m
(a) CH_4/air
(b) C_3H_8/air

5cm×5cm×1.8m
(c) CH_4/air
(d) C_3H_8/air

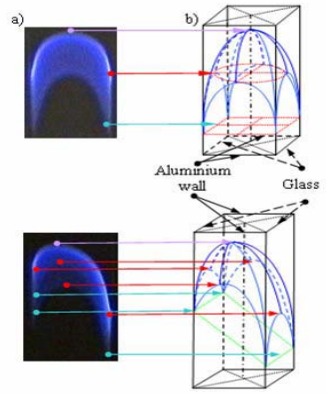

Figure 16. The surface flame shapes in the C_3H_8/air mixture during propagation in flammability column
(a) camera pictures; top: stable and bottom: unstable;
(b) 3-D model of the flame surfaces.

The last important factor affecting the quality PIV pictures of the recorded velocity fields, worth further processing, is the laser light impulse energy used in particular experiment. In general, this is connected with the seed numbers "seen" by the camera which depends upon the "sheet laser light" thickness. The latter grows with energy impulse and with the distance between the laser and the analyzed object. Fig. 17 shows two examples of pictures chosen from a big number stored. The top row pictures show: too high impulse and too small seed mass. Usually there is a trade off between these factors in order to achieve their combination resulting in the best, optimal final effect.

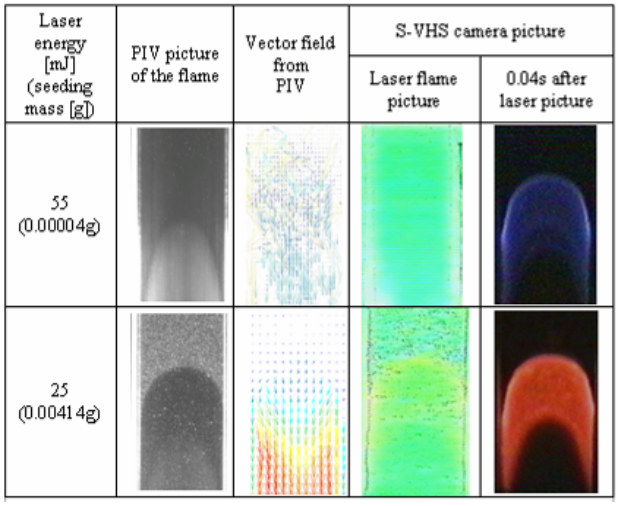

Figure 17. Influence of the laser energy impuls and the seeding mass on the PIV flame and velocity field pictures quality. The flame propagates in the C_3H_8/air mixture. The total mass of the MgO seeding in the column are given.

RESULTS

When the setting of all the parameters is correct full set of the PIV data is produced. A small example is shown in Fig.18. The flame stretch rate has been calculated for both mixtures.

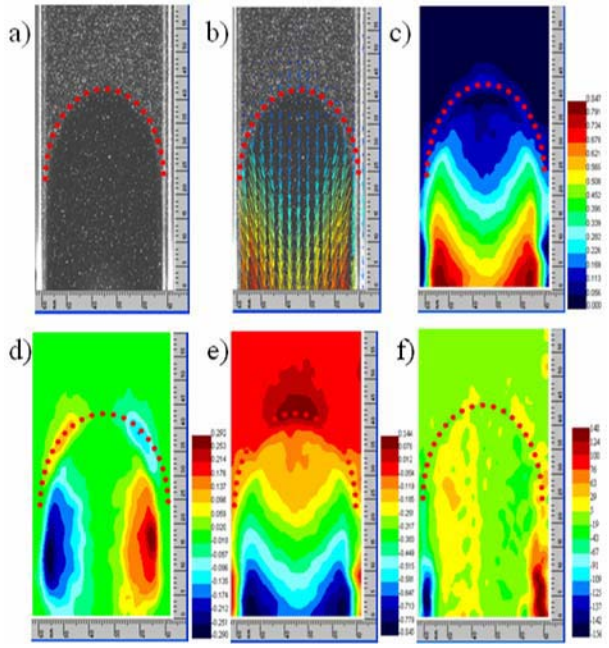

Figure 18. The PIV flame propagation velocity pictures. Its position is additionally marked by red dots.
The C_3H_8/air mixture; column: 5cm×5cm×1.8m.
(a) single PIV picture showing seeding; (b) velocity field; (c) total velocity V_c [m/s]; (d) V_x component [m/s]; (e) V_z component [m/s]; (f) flow rotation.

The important relations related to the theory are given below. The flame stretch rate k [s^{-1}] is determined by the formula [7]:

$$k=\frac{1}{A}\cdot\frac{dA}{dt} \tag{4}$$

where: A – flame area and t – time

The stretch affects laminar flame velocity and this effect is expressed by the equation [8]:

$$u_L = u_{L\infty} - k\,L_M \tag{5}$$

The last equation can be written also as the Markstein length L_M definition. It can be also rearranged to the following formula

$$u_L / u_{L\infty} = 1 + Ma\,Ka \tag{6}$$

where: $Ka = k\cdot\delta/u_L$ – the Karlowitz number
$Ma = L_M/\delta$ – the Markstein number

It is worth noticing that the flame thickness δ used in Ka and Ma numbers is defined as

$$\delta = D_m/u_L = \delta_{Zel}/Le \tag{7}$$

where $$Le=a_m/D_m \tag{8}$$

Only for $Le=1$ one obtains $\delta=\delta_{Zel}$, and no other flame thickness definitions presented earlier are involved in these considerations.

The flame stretch rate calculation in a standard flammability column case is considered as the main goal of this paper. It can be determined by utilizing the PIV-method to obtain the velocity field. For 2-D case, and coordinates bound to moving flame, this stretch can be calculated by the expression ([9], [10], [11] and Fig.19).

$$k = \frac{dV_t}{dL} + \frac{V_t\cdot\cos\varphi}{\ell} \tag{9}$$

where: L – length along flame surface;
V_t – tangential velocity of the chosen point
φ – angle defining the chosen point with velocity V_t
l – distance of the point from the column symmetry axis.

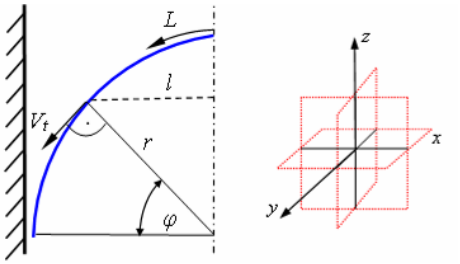

Figure 19. Definition of parameters for calculation of the local stretch flame k along the flame front L.

All quantities in the Eq. 9 have been calculated using MathCad. Results, for both lean mixtures, i.e. CH_4/air and C_3H_8/air, are shown in Figs 20 and 21, respectively.

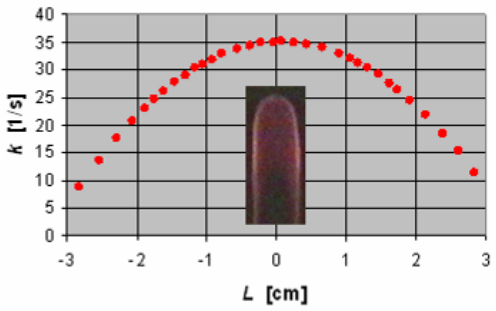

Figure 20. Local stretch rate k along flame front L: the lean CH_4/air 5.25% mixture; column: 5cm×5cm×1.8m.

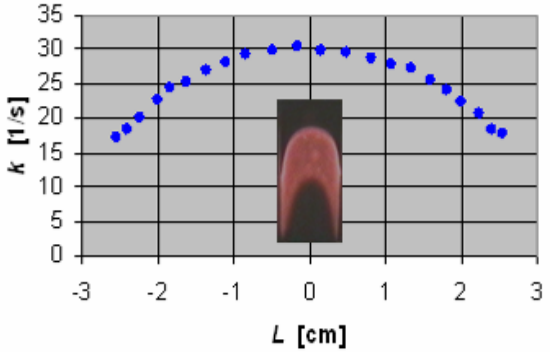

Figure 21. Local stretch rate k along flame front L: the lean C_3H_8/air mixture; column 5cm×5cm×1.8m.

The PIV measurement results show that local stretch rate is maximum at the flame top for both cases. This is in line with earlier empirical and numerical modeling results. The results also agree also with observations that extinction of upward propagating limit flame starts at its tip. Apart from results presented above, it is worth showing two PIV pictures related to this flame extinction process and velocity field associated with it. Both are shown in Figs 22 and 23, respectively, and support above statements.

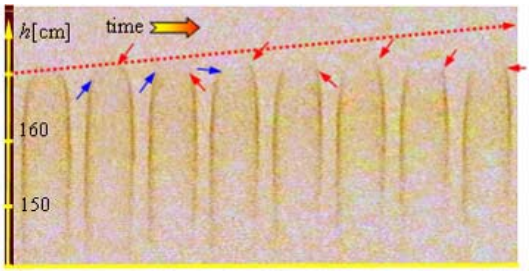

Figure 22. The extinction process pictures of the upward propagating flame (close to the 5cm×5cm×1.8m column top end) in the CH_4/air 5.25% mixture. Pictures (presented as negatives) were taken at 0.02s intervals.

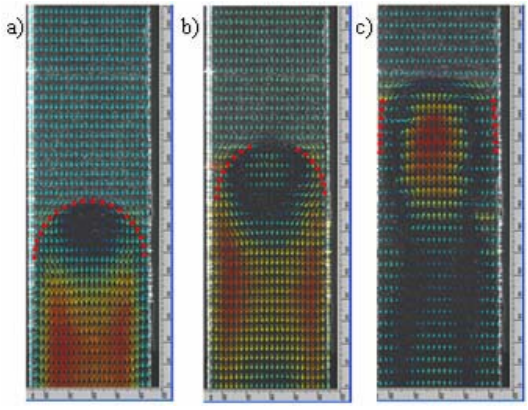

Figure 23. PIV vector velocity fields of the flame extinction process, propagation in the flammability column, CH_4/air mixture. Fields shown in coordinate system bound to the moving flame. The time interval between shown pictures 0.25s. Flame position is additionally marked by red dots.

CONCLUSION

The flame velocity fields in lean limit CH_4/air and C_3H_8/air mixtures, propagating upward in a standard flammability column, were experimentally studied using PIV-method. The local stretch rate distribution in these mixtures (along the flame front), using PIV measurements data, were determined. For both cases the maximum value is at the flame leading point. The PIV velocity fields related to 2 important cases, i.e. (1) the flame extinction process and (2) existence of the combustion products region, in lean limit CH_4/air mixture, situated below the flame tip and moving with the same velocity as the flame – are also presented. The methodology of PIV measurements is also described. It addresses: (i) the maximum MgO seeding mass in the mixture without any effect on the laminar flame propagation; (ii) the range of minimum and maximum laser light energy impulse which gives good quality to all PIV pictures (i.e. recorded ones and resulted from further processing), (iii) the condition of the stable flame propagation in the column and (iv) the comparison of and support to the PIV-pictures, the ones obtained by the ”shadow”-method and relevant to present paper.
This work is in progress and further detailed analyses will follow.

ACKNOWLEDGMENTS

Results presented in the paper are from currently conducted projects supported by EU Marie Curie ToK ECHTRA (Nr 509847) and also by Technical University of Lodz, Faculty of Engineering, KTCiCH (Nr K-15/701/BW and Nr K-15/699/DzS).

REFERENCES

[1] Karlovitz, B., Denniston, D.W., Knapschaefer, D.H., and Wells, F.E., Proc. Combust. Inst. 4 (1953) 613-620;
[2] Jarosiński J.: *Techniki czystego spalania*, (in Polish), WNT, Warszawa 1996;
[3] Spalding, D.B. Combust. Flame, 1, 296, 1957;
[4] Zeldo'vich, Ya. B.: *Tieorija gorenija i dietonacji gazow*, (in Russian) Moscow, 1944;
[5] Gaydon A. G., Wolfhard H. G.: *Flames-their structures, radiation and temperature,* Chapman and Hall, London, 1953;
[6] Andrews G. E., Bradley D.: *The burning velocity of methane-air mixtures*, Combustion and Flame 19, 1972, pp. 275-288;
[7] Ronney, P. D.: *Premixed-gas flames,* in: Microgravity combustion: Fires in free fall, (Ross H. D.), Academic Press, London, U. K., 2001, pp. 35-82;
[8] Kwon S., Tseng L. K., Faeth G. M.: *Laminar burning velocities and transition to unstable flames in $H_2/O_2/N_2$ and $C_3H_8/O_2/N_2$ mixtures*, Combustion and Flame 90, 1992, pp. 230-246;
[9] Von Lavente E. and Strehlow R. A.: *The mechanism of lean limit flame extinction,*Combustion and Flame 49,1983,pp. 123-140;
[10] Jarosinski J., Podfilipski J. and Fodemski T.: *Properties of flames propagating in propane-air mixtures near flammability and quenching limits*, Combust. Sci. and Tech.,174; 2002, pp. 167-187;
[11] Shoshin Y., Gorecki G., Jarosinski J. and Fodemski T.: *Experimental study of lean limit methane/air flame in a standard flammability tube using particle image velocimetry method*, article accepted for publication in Combustion and Flame 2008.